



# The effect of the series resistance on the photovoltaic properties of In-doped CdTe(*p*) thin film homojunction structure

W.F. Mohamed\*, Maan Ahmed Shehathah

*Electrical Engineering Department, University of Mosul, Mosul, Iraq*

Received 5 January 2000; accepted 10 January 2000

---

## Abstract

The photovoltaic properties of In-doped CdTe(*p*) thin film homojunction structure have been investigated; the effect of the series resistance on the short circuit current has especially been discussed in detail. A simulation of the fabricated device is achieved successfully using the PSPICE computer program. Mathematical derivations are implemented in order to interpret the results. It is found that the deteriorative effect of the series resistance on the short circuit current vs light intensity characteristics increases by increasing the light intensity. A new factor has been suggested to be a measure of how the series resistance affects the solar cell behavior at low and high light intensities. © 2000 Published by Elsevier Science Ltd. All rights reserved.

---

## 1. Introduction

CdTe thin films have attracted attention for their potential applications in the areas of solar energy conversion, gamma ray detection, and electrooptic modulator, due to their low thermal noise and large absorption coefficient [1]. A significant conversion efficiency of light into electricity has been achieved using CdTe solar cells. Recently, a photovoltaic conversion efficiency of 16% has been measured. CdTe has the advantage of a nearly ideal band gap for solar cell

---

\* Corresponding author.

terrestrial photoconversion (1.5 eV), a sharp optical absorption edge, and large absorption coefficients and tolerance for relatively short minority carrier diffusion in the material [2].

The effect of Indium doping on the electrical characteristics of CdTe thin film has been studied for many years [3]. Recently Hussain et al. [4] revealed the possibility of controlled doping with Indium for net donor concentration between  $10^{15}$  and  $10^{18} \text{ cm}^{-3}$  in CdTe, using an annealing temperature as a control factor.

One of the important parameters that affect solar cell performance is the series resistance. As a practical matter it is generally found that the series resistance in a cell should be no more than a few tenths of an ohm for each square centimeter of illuminated cell area under one sun condition. If this is exceeded the cell loads itself down with internal resistance [5]. The series resistance becomes more effective at high light intensities due to the high photocurrent generated [6].

In this paper we shall study the photovoltaic properties of In-doped CdTe(*p*) thin film, and the effect of the series resistance ( $R_s$ ) on the short circuit current ( $I_{sc}$ ) and the possibility of using this device as a solar cell.

## 2. Solar cell model characterization

Since the solar cell is a semiconductor diode (without illumination), it has the characteristics of the pn junction, hence its dark current ( $I_d$ ) can be given as [6]:

$$I_d = I_0(e^{(V_d/nV_t)} - 1) \quad (1)$$

where  $I_0$  is the saturation current,  $V_d$  is the voltage applied across the junction,  $n$  is the ideality factor, and  $V_t$  is the thermal voltage (0.026 V) at 300 K.

During illumination, minority carriers will flow across the junction producing a photocurrent ( $I_{ph}$ ). The flow of this photocurrent in external electrical load will produce a forward voltage across the cell terminals. Due to this forward bias voltage more majority carriers will cross the junction, producing a dark current which will flow in the opposite direction to the photocurrent.

Dark current can be due to injection of carriers, recombination within the depletion region, and a tunneling effect. If the injection current is predominant, then the ideality factor is one; otherwise, the ideality factor must be taken to be greater than one.

A solar cell model can be considered, as shown in Fig. 1, taking into account the effect of the series resistance ( $R_s$ ) and shunt resistance ( $R_{sh}$ ) [7]. The current supplied to the load ( $I$ ) can be expressed as:

$$I = I_{ph} - I_d - I_{sh} \quad (2)$$

where  $I_{sh}$  is the current flowing through the shunt resistance. By substituting the dark current in Eq. (1) and  $I_{sh} = (V_d/R_{sh}) = (V + IR_s)/R_{sh}$ , since  $V_d = V + IR_s$ , where  $V$  is the voltage across the load ( $R_L$ ), Eq. (2) can be written in the form:

$$I = I_{ph} - I_0(e^{(V+IR_s)/nV_t} - 1) - \frac{(V + IR_s)}{R_{sh}} \quad (3)$$

$I_{ph}$ ,  $I_0$ ,  $R_{sh}$ , and  $R_s$  are calculated practically and fed into the PSPICE program in order to characterize the other solar cell parameters.

### 2.1. Solar cell parameters calculations

Photons are the means by which energy is transferred into the cell. Ideally, each photon above a certain threshold energy is absorbed by creating an electron-hole pair that gives rise to a single electron flowing in the external circuit. The short circuit current depends upon the rate of generation of minority carriers within the cell and the fraction of minorities that diffuse to the junction and are collected. Theoretically, the short circuit current is equal to the photocurrent [7]. The photocurrent density ( $J_{ph}$ ) can be given as [8]:

$$J_{ph} = qF(1 - R)(1 - e^{-\alpha W})\eta \quad (4)$$

where  $q$  is the electronic range,  $F$  is the number of incident photons with energies greater than the band gap energy ( $E_g$ ) in [ $\text{cm}^{-2} \text{s}^{-1}$ ] units,  $R$  is the reflection coefficient,  $\alpha$  is the absorption coefficient [ $\text{cm}^{-1}$ ],  $W$  is the thickness of the cell [ $\text{cm}$ ], and  $\eta$  is the collection efficiency.

In general, most of the above parameters are a function of wavelength of the incident photons, ( $\lambda$ ). Thus, a more complete equation of photocurrent density would be:

$$J_{ph} = q \int_{\lambda} F(\lambda)(1 - R(\lambda))(1 - e^{-\alpha(\lambda)W})\eta(\lambda)d\lambda \quad (5)$$

The series resistance of a solar cell represents the sum of all resistance elements distributed in the semiconductor, the ohmic contacts, the semiconductor contact interfaces, and the bulk resistance of the base [9]. Since the measured value of the bulk resistivity of the prepared CdTe film is very high ( $10^8 \Omega \text{cm}$ ), we shall assume

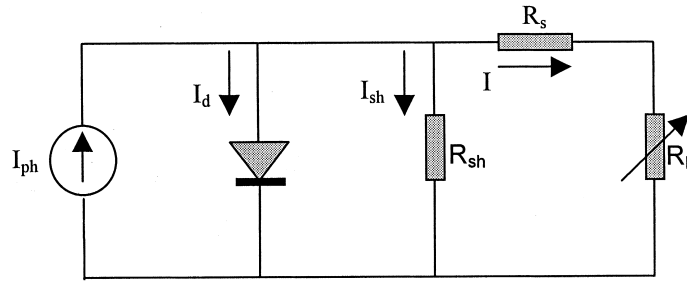


Fig. 1. Solar cell model.

that the series resistance is approximately equal to the bulk resistance of the CdTe thin film.

The saturation current ( $I_0$ ) can be estimated from d.c. measurements of the forward-biased diode characteristic [10]. By taking the natural logarithm of the two sides of Eq. (1), at high diode current values, it becomes:

$$\ln(I_d) \approx \ln(I_0) + \frac{V_d}{nV_t} \quad (6)$$

However, the ideal saturation current can be determined by extrapolating the vertical axis for the  $\ln(I_d)$  vs  $V_d$  characteristics.

### 3. Experimental details

A few samples of the structure In–In-doped CdTe(*p*)–Al were prepared by vacuum evaporation technique using Balzers unit (BA-510) as a coating system. A thin aluminum layer (2000 Å) was deposited on a micro-glass slide, followed by the evaporation of the CdTe layer under a vacuum of  $8 \times 10^{-6}$  mbar at a substrate temperature  $T_s = 25^\circ\text{C}$ , and at 20 Å/s rate of deposition with a thickness of 16,584 Å (1.6584 μm). The deposited CdTe layer was then annealed at 350°C for half an hour under vacuum (since the annealing process promotes the *p*-type of the evaporated CdTe thin film [11]). Then an Indium layer of 100 Å was deposited on the CdTe layer to be diffused later by an annealing process under vacuum, and at 85°C annealing temperature for 1 h, in order to form an In-doped CdTe(*p*) homojunction structure (see Fig. 2). The top contact was then formed by depositing a thin layer of Indium (4000 Å) in grid form.

### 4. Results and discussion

Fig. 3 illustrates the (*I*–*V*) characteristics of the fabricated device. It is clear that the forward current is low and bent towards the voltage axis, which is attributed to the high series resistance [2].

The device has shown an open circuit voltage of 180 mV at 100 mW/cm<sup>2</sup> light intensity, and a low short circuit current ( $I_{sc}$ ). Fig. 4 shows the variation of the

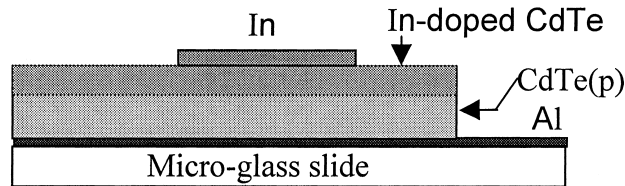
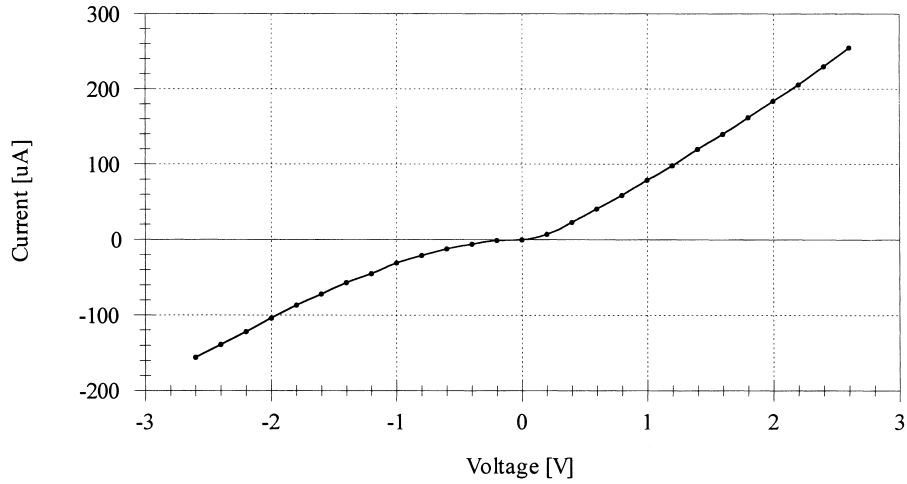


Fig. 2. A cross section of the fabricated device.

Fig. 3. The (I–V) characteristic of In-doped CdTe(*p*).

short circuit current with the light intensity that measured practically. The low short circuit current is due to the high bulk resistivity ( $\rho_b$ ) of the prepared film from which the bulk resistance can be calculated using the equation:

$$R_b = \rho_b \frac{W}{A} \quad (7)$$

where  $R_b$ ,  $A$ , and  $W$  are the bulk resistance, the area, and the thickness of the device, respectively. Knowing that  $A = 1 \text{ cm}^2$ ,  $W = 1.6583 \text{ } \mu\text{cm}$ , and  $\rho_b = 10^8 \text{ } \Omega$

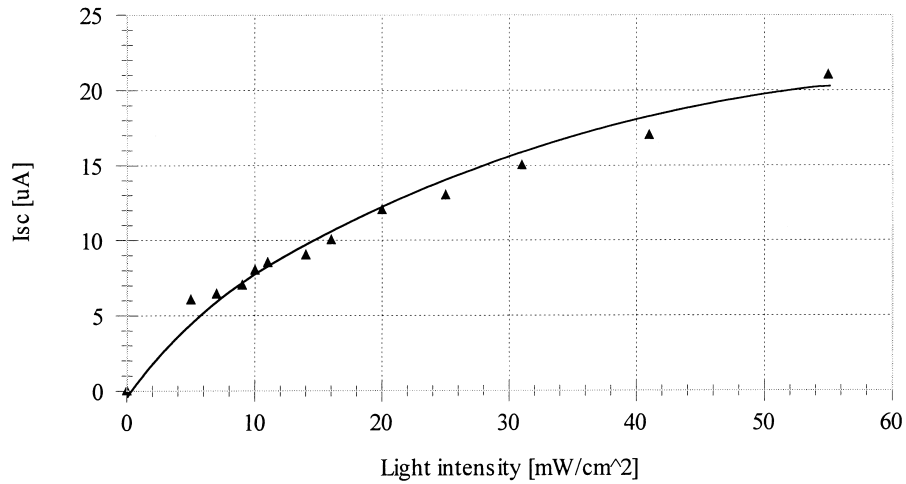


Fig. 4. The short circuit current vs light intensity characteristics.

cm, hence the value of the bulk resistance is 16.584 k $\Omega$  which is a very high resistance. However, it may be considered the dominant resistance compared with the low contact resistances, so the series resistance may be approximately equal to the bulk resistance.

By looking at Fig. 4, two regions can be recognized. That is, in the light intensity range (0–6 mW) the short circuit current varies more rapidly than that in the range (6–60 mW). In other words, the increment in the short circuit current ( $\Delta I_{sc}$ ) tends to decrease with the increase in the light intensity. It is suggested that this degradation in the cell performance at high light intensities is due to the high series resistance.

In order to investigate the effect of the series resistance on the short circuit current at low and high light intensities, the solar cell model, shown in Fig. 1, will be analyzed by the PSPICE computer program.

#### 4.1. Solar cell modeling by PSPICE

Today, SPICE is the circuit simulator most designers are familiar with. PSPICE can be regarded as a standard in circuit simulation [10]. In order to simulate the solar cell model the various circuit parameters must be determined. It is found that the series resistance ( $R_s$ ) is equal to 16.584 k $\Omega$ , as mentioned in Section 4, the saturation current ( $I_0$ ) is found in Fig. 5, and it is equal to 24  $\mu$ A. The shunt resistance ( $R_{sh}$ ) is considered to be variable. The ideality factor ( $n$ ) is assumed to be equal to two. The photocurrent ( $I_{ph}$ ) is calculated numerically from Eq. (5) with the help of the MATLAB program. It is clear that the  $I_{ph}$  depends on  $R(\lambda)$ ,  $\alpha(\lambda)$ , and  $F(\lambda)$ , as explained in Eq. (5). The collection efficiency  $\eta(\lambda)$  has been varied in order to calculate the variation in  $I_{ph}$ ; it is found that when the

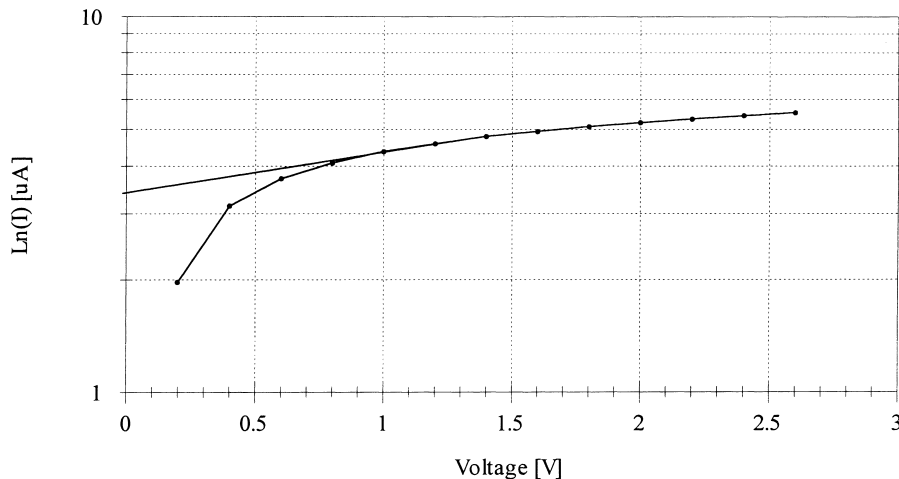


Fig. 5. The (ln(I)–V) characteristics.

collection efficiency varies from 0 to 1, the photocurrent varies from 0 to 37.3 mA (keeping in mind that the area of the device is  $1 \text{ cm}^2$ ). It is worth mentioning that the limits of integration in Eq. (5) are from 0.45 to  $0.82 \text{ }\mu\text{m}$  (i.e. to the cutoff wavelength, which is equal to  $0.82 \text{ }\mu\text{m}$  for the band gap of the CdTe ( $E_g = 1.5 \text{ eV}$ ), above which the absorption process can be ignored).

The reflection coefficient of the fabricated cell is measured as a function of the light wavelength using spectrophotometer, as shown in Fig. 6. It is clear that the reflection coefficient is constant and has a minimum value in the range 0.45 to  $0.55 \text{ }\mu\text{m}$  wavelength and it has a maximum value in the range  $0.7$  to  $0.8 \text{ }\mu\text{m}$ , while it is varied in the range  $0.5$  to  $0.7 \text{ }\mu\text{m}$ .

The absorption coefficient for the *p*-type CdTe thin film is taken from Ref. [11] and shown in Fig. 7. It is seen that the absorption coefficient decreases with the increase in the light wavelength and the CdTe has a sharp absorption edge. Also, the spectral photon irradiance is measured experimentally as a function of the light wavelength, as shown in Fig. 8.

#### 4.2. Mathematical derivations

From the above measurements, Figs. 6–8, and using Eq. (5),  $I_{ph}$  has been calculated. Using the PSPICE program, the variation of short circuit current ( $I_{sc}$ ) with photocurrent ( $I_{ph}$ ) has been calculated and drawn, as shown in Fig. 9, for different shunt resistances ( $R_{sh}$ ), and keeping the value of the series resistance constant with a value  $16.584 \text{ k}\Omega$ . Fig. 9 must be studied carefully because it represents the most important results in this paper.

The results obtained in Fig. 9 are approximately similar to that obtained practically in Fig. 4 for high values of the shunt resistance [since the photocurrent

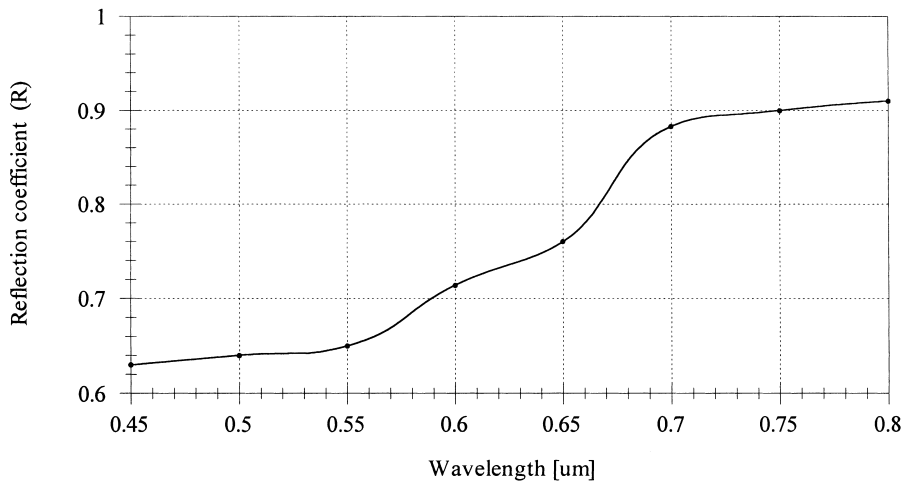


Fig. 6. The reflection coefficient vs wavelength characteristics.

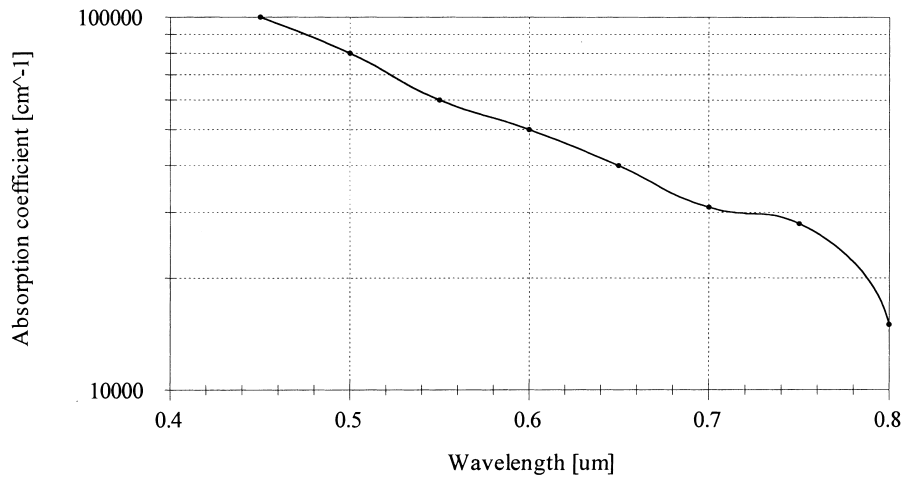


Fig. 7. The absorption coefficient vs wavelength characteristics.

is proportional to the spectral photon irradiance as in Eq. (4), which in turn is proportional to the light intensity].

With the help of Eq. (3), at short circuit current condition, the voltage ( $V$ ) across the load resistance ( $R_L$ ) becomes zero, so Eq. (3) can be written as:

$$I_{sc} = I_{ph} - I_0 [e^{(I_{sc} R_s / n V_t)} - 1] - \frac{I_{sc} R_s}{R_{sh}} \quad (8)$$

By mathematical manipulations of Eq. (8), an expression for  $(dI_{sc}/dI_{ph})$  can be

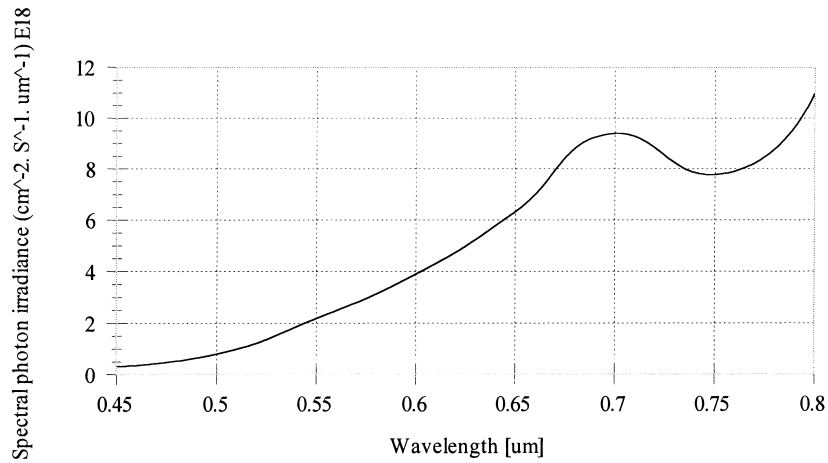


Fig. 8. The spectral photon irradiance.



given as:

$$\frac{dI_{sc}}{dI_{ph}} = \frac{1}{\left[1 + \frac{R_s}{R_{sh}}\right] + \left[\frac{I_0 R_s}{n V_t} e^{(I_{sc} R_s / n V_t)}\right]} \quad (9)$$

Looking back to the results obtained in Fig. 9, it can be seen that there are two regions in the curve for each value of the shunt resistance. One of which is of a high slope (and approximately constant) at low photocurrent values, and the other is of a lesser slope (and slightly variable) at higher photocurrent values. Using these two regions we compared them with Eq. (9). Its denominator is composed of three terms. The first and the second terms represented a constant part (do not vary with  $I_{sc}$ ), while the third term is variable (vary with  $I_{sc}$ ). So, at very low  $I_{sc}$ , the constant term becomes much greater than the variable term, which is expressed as:

$$1 + \frac{R_s}{R_{sh}} \gg \frac{I_0 R_s}{n V_t} e^{(I_{sc} R_s / n V_t)} \quad (10)$$

then the slope can be approximated to:

$$\frac{dI_{sc}}{dI_{ph}} = \frac{1}{\left(1 + \frac{R_s}{R_{sh}}\right)} = \frac{R_{sh}}{R_{sh} + R_s} \quad (11)$$

At high values of  $I_{sc}$ , the variable term becomes much greater than the constant term, which is expressed as:

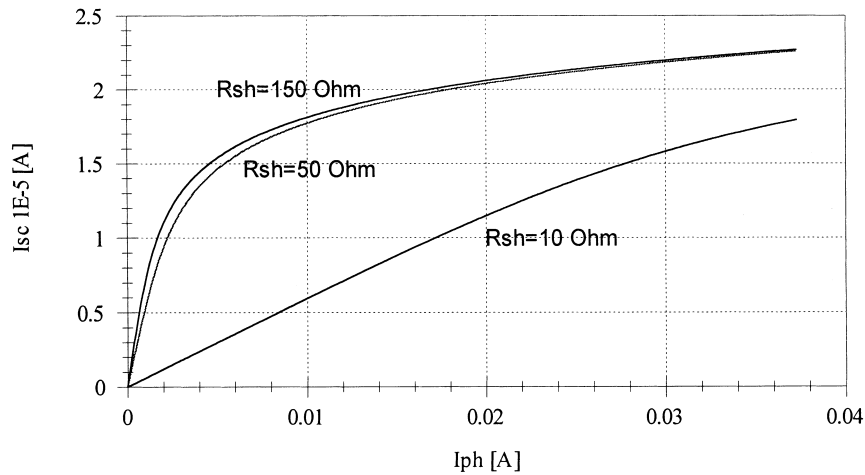


Fig. 9. The ( $I_{sc}$ – $I_{ph}$ ) characteristics for different shunt resistances.

$$1 + \frac{R_s}{R_{sh}} \ll \frac{I_0 R_s}{n V_t} e^{(I_{sc} R_s / n V_t)} \quad (12)$$

then the slope can be approximated to:

$$\frac{dI_{sc}}{dI_{ph}} = \frac{1}{\frac{I_0 R_s}{n V_t} e^{(I_{sc} R_s / n V_t)}} \quad (13)$$

It becomes obvious that at low photocurrent (low light intensity), the short circuit current variations depend mainly on the shunt resistance. Also, the slope of the curve increases as the shunt resistance increases. But the interval between one curve and the other is decreased as the shunt resistance increases; this is due to the limited value of the photocurrent supplied (see Fig. 1).

The above result can be interpreted and agreed with Eq. (11) by keeping the series resistance constant.

Fig. 10, which is obtained by simulation, shows the  $(I_{sc}-I_{ph})$  characteristics for different values of the series resistance, with shunt resistance of an arbitrary value  $R_{sh}=1 \text{ k}\Omega$ . It has been explained that Eq. (13) is derived at high light intensities (high photocurrents), which in turn means high short circuit currents, but it can be seen from Eq. (13) that the slope varies inversely with  $(I_0 R_s / n V_t) \exp(I_{sc} R_s / n V_t)$  that means the variation of  $I_{sc}$  will be less as the  $I_{ph}$  increases due to the high effect of  $R_s$  that is evident in Fig. 10.

To estimate the value of the short circuit current ( $I_{sc}$ ) below which the slope becomes constant, we solve Eq. (10) for  $I_{sc}$ . In order to deal with this equation, it may be convenient to rewrite it in the following acceptable form:

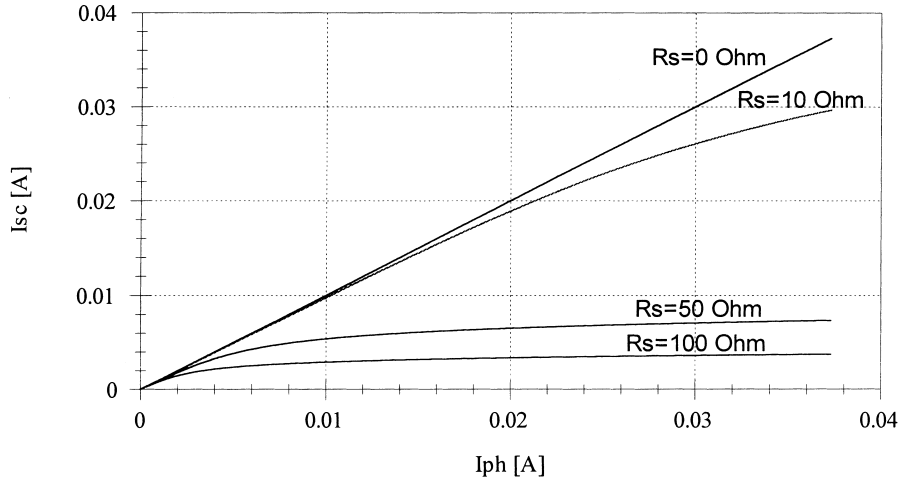


Fig. 10. The  $(I_{sc}-I_{ph})$  characteristics for different series resistances.

$$1 + \frac{R_s}{R_{sh}} \geq 10 \times \frac{I_0 R_s}{n V_t} e^{(I_{sc} R_s / n V_t)} \quad (14)$$

Solving ( $I_{sc}$ ), we get:

$$I_{sc} \leq \frac{n V_t}{R_s} \ln \left[ \frac{n V_t}{10 I_0 R_s} \left( 1 + \frac{R_s}{R_{sh}} \right) \right] \quad (15)$$

In order to investigate the validity of Eq. (15), Table 1 is constructed, which illustrates the values of short circuit current ( $I_{sc}$ ) for different shunt resistances, below which the slope is constant as measured from Fig. 9. Also, it includes the corresponding values of the ( $I_{sc}$ ) that was calculated from Eq. (15). It is obvious that the theoretical values are in good agreement with that obtained by simulation.

#### 4.3. Definition of a “short circuit current degradation factor”

When the value of the series resistance ( $R_s$ ) is zero, the short circuit current ( $I_{sc}$ ) will be equal to the photocurrent ( $I_{ph}$ ) (see Fig. 1). That is, the slope ( $dI_{sc}/dI_{ph}$ ) will be equal to one (we can stress the validity of Eq. (9) by substituting  $R_s=0$  which gives a slope equal to one). As the series resistance increases, its deteriorative effect on the short circuit current will be increased, especially at high light intensities. Here, it is very important to define a “**short circuit current degradation factor**”. This factor gives a fraction by which the increment in the short circuit current ( $\Delta I_{sc}$ ), relative to the photocurrent increment ( $\Delta I_{ph}$ ), is reduced due to the existence of the series resistance. However, it can be assigned as “ $S$ ” and expressed as the ratio of the slope  $\Delta I_{sc}/\Delta I_{ph}$  at  $R_s > 0$  to the same slope, but with  $R_s=0$ , which can be written as:

$$S = \frac{\left[ \frac{\Delta I_{sc}}{\Delta I_{ph}} \right]_{R_s \neq 0}}{\left[ \frac{\Delta I_{sc}}{\Delta I_{ph}} \right]_{R_s = 0}} \quad (16)$$

Since  $\Delta I_{sc}/\Delta I_{ph}$  at  $R_s=0$  is equal to one, hence the above equation can be given by:

Table 1

The measured and calculated values of short circuit current ( $I_{sc}$ ) for different values of shunt resistance

$R_s$ [k $\Omega$ ]	$R_{sh}$ [ $\Omega$ ]	$I_{sc}$ (measured from simulation curves shown in Fig. 9) [ $\mu$ A]	$I_{sc}$ [calculated from Eq. (15)] [ $\mu$ A]
16.584	10	9	9.6
16.584	50	4.4	4.6
16.584	150	1.1	1.18

$$S = \frac{dI_{sc}}{dI_{ph}} = \frac{1}{\left[1 + \frac{R_s}{R_{sh}}\right] + \left[\frac{I_0 R_s}{n V_t} e^{(I_{sc} R_s / n V_t)}\right]} \quad (17)$$

However, the values of this factor is bounded in the range 0 to 1, that is, when the series resistance is zero then  $S = 1$  (the ideal case), and when the series resistance is infinite then  $S = 0$  (open circuit case).

## 5. Conclusions

The In-doped CdTe(*p*) thin film prepared by vacuum evaporation is of high bulk resistivity about ( $10^8 \Omega \text{ cm}$ ). The high resistivity largely affects the thin film photovoltaic properties, particularly the short circuit current. The deteriorative effect of the series resistance increases by increasing the light intensity, which in turn limits the benefit of using the light concentrators that improve the short circuit current. Mathematical derivations, that depict the effect of the series and shunt resistances on the short circuit current at low and high light intensities, have been shown to be valid and can be applied to the solar cell model that has been studied and discussed in this research.

## References

- [1] Kim MD, Kang TW, Han MS, Kim TW. Rapid thermal annealing effects in CdTe (111) thin films grown on GaAs (100) substrates. *Jpn J App Phys* 1996;35:4220–4.
- [2] Al-Dhafri AM. Photovoltaic properties of CdTe–Cu<sub>2</sub>Te. In: *Proceedings of the Sixth Arab International Solar Energy Conference, AISEC-6, Muscat, Sultanate of Oman, 29 March–1 April, 1998*.
- [3] Watson E, Shaw D. The Solubility and Diffusivity of In in CdTe. *J Phys C: Solid State Phys* 1983;6:515–37.
- [4] Hussain AA, Luqman SA. Characterization of In-doped CdTe thin film. *Mu'tah Journal for Research and Studies* 1996;11(5):207–18.
- [5] Fonash ST. *Solar cell device physics*. Academic Press, 1981.
- [6] Younis MA. *Theoretical Investigation of the Efficiency of Silicon Solar Cell*. M.Sc. thesis, University of Musol, College of Engineering, 1985.
- [7] Vian HA. *Effect of the Junction Depth and the Lifetime of the Minority Carriers on the Performance of the Solar Cell*. M.Sc. thesis, University of Musol, College of Science, 1998.
- [8] William CD, Paul NC. *Solar energy handbook*. Marcel Dekker, 1980.
- [9] Anwar SH. *Improved Efficiency Cu<sub>2</sub>S/CdS Thin Film Heterojunction Solar Cell*. M.Sc. thesis, University of Musol, College of Engineering, 1984.
- [10] Paola A, Giuseppe M. *Semiconductor device modeling with SPICE*. McGraw-Hill, 1988.
- [11] Ou SS, Stufsudd OM. Optical properties of electrochemically deposited CdTe films. *J App Phys* 1984;55(10):3769–72.